THE JOURNAL OF BIOLOGICAL CHEMISTRY VOL. 285, NO. 51, pp. 39898–39904, December 17, 2010

Structure of Human Stabilin-1 Interacting Chitinase-like Protein (SI-CLP) Reveals a Saccharide-binding Cleft with Lower Sugar-binding Selectivity*[S]

Received for publication, April 5, 2010, and in revised form, August 15, 2010 Published, JBC Papers in Press, August 19, 2010, DOI 10.1074/jbc.M110.130781

Geng Meng[‡§], Yanmei Zhao[‡§1], Xiaoyun Bai[‡§], Yong Liu[‡§], Todd J. Green[¶], Ming Luo[¶], and Xiaofeng Zheng[‡§2]

From the [‡]National Laboratory of Protein Engineering and Plant Genetic Engineering, [§]Department of Biochemistry and Molecular Biology, College of Life Sciences, Peking University, Beijing 100871, China and the [¶]Department of Microbiology, University of Alabama at Birmingham, Birmingham, Alabama 35294

Human secreted protein stabilin-1 interacting chitinase-like protein (SI-CLP) has been identified as a novel member of Glyco_18 domain-containing proteins that is involved in host defense and inflammatory reactions. Efficient secretion of SI-CLP is mediated by its interaction with the endocytic/sorting receptor stabilin-1. SI-CLP is expressed abundantly in macrophages and neutrophils and is up-regulated by Th2 cytokine IL-4 and glucocorticoid, which suggest that SI-CLP could be a marker for adverse effects of glucocorticoid therapy. To gain insight into the biological function of SI-CLP, we determined the crystal structure of SI-CLP at 2.7 Å resolution by x-ray crystallography and found that it featured a typical triose-phosphate isomerase barrel fold with a putative saccharide-binding cleft. Comparison with other chitinase-like proteins showed the cleft to be atypically wide and open. The saccharide-binding capacity of SI-CLP was investigated, and its ligand-binding specificity was found to relate to the length of the oligosaccharides, with preference for chitotetraose. Further investigations reveal that SI-CLP could bind LPS *in vitro* and neutralize its endotoxin effect on macrophages. Our results demonstrate the saccharide-binding property of SI-CLP by structure and *in vitro* biochemical analyses and suggest the possible roles of SI-CLP in pathogen sensing and endotoxin neutralization.

The mammalian family of Glyco_18 domain-containing proteins comprises enzymatic activated chitinases and chitinase-like proteins lacking chitinase activity. Each protein in this family contains a Glyco_18 domain comprising a triose-phosphate isomerase (TIM)[3] barrel fold that holds lectin properties with specific sugar-binding preference. Among these, true enzymes such as acidic mammalian chitinase and chitotriosidase each have an additional chitin-binding domain and are shown to hydrolyze chitin (1, 2). YKL39, YKL40 (also named HCgp39), and mouse YM1/2 are the chitinase-like proteins that lack chitin hydrolysis activity (3–5). Although the chitinase-like proteins have no enzyme activity, accumulated data suggest that these proteins possess the lectin property. YKL40 was proved to bind chitin fragment (3), YM1 preferentially binds saccharides with a free amine group, such as glucosamine (GlcN) or galactosamine (GalN) polymers, instead of chitin fragment (6). Besides, the chitinase-like proteins are also biomarkers for various human diseases (7).

The recently identified stabilin-1 interacting chitinase-like protein (SI-CLP) is a human secreted protein that belongs to the family of chitinase-like proteins, based on the NCBI annotation. SI-CLP was detected abundantly in bronchoalveolar lavage from patients with chronic inflammatory disorders of the respiratory tract, human peripheral blood leukocytes, and patients undergoing glucocorticoid therapy(8). Efficient secretion of SI-CLP is mediated by its interaction with the endocytic/sorting receptor stabilin-1 and is activated by Th2 cytokines (8). Our recent work detected the existence of SI-CLP in the synovial fluid of patients with osteoarthritis or rheumatoid arthritis and found that administration of SI-CLP increased the severity of inflammation in collagen-induced arthritis rat. Full-length SI-CLP contains 393 amino acids with a signal peptide at its N terminus and a predicted Glyco_18 domain. But the sequence identity between SI-CLP and any other Glyco_18 domain proteins is below 20%, and general sequence alignment between SI-CLP and other chitinase-like proteins could not provide any useful information. As a member of chitinase-like protein, SI-CLP has no chitin-hydrolyzing activity. No evidence so far shows that SI-CLP possesses lectin property, and the precise physiology function of SI-CLP is still unknown.

To gain insight into the biological function of SI-CLP, we determined the crystal structure of full-length SI-CLP and identified a putative saccharide-binding site in the Glyco_18 domain of SI-CLP. Structure superimposition-based sequence

* This work was supported by National Science Foundation of China Grant 30870487, National Basic Research Program of China 973 Program Grant 2010CB911800 and 863 Program Grant 2006AA02A314, and the International Centre for Genetic Engineering and Biotechnology Project CRP/CHN09-01. Portions of this research as x-ray diffraction data collection were carried out at the Stanford Synchrotron Radiation Laboratory, a national user facility operated by Stanford University on behalf of the U.S. Department of Energy, Office of Basic Energy Sciences.

[S] The on-line version of this article (available at http://www.jbc.org) contains supplemental Figs. 1 and 2.

The atomic coordinates and structure factors (code 3BXW) have been deposited in the Protein Data Bank, Research Collaboratory for Structural Bioinformatics, Rutgers University, New Brunswick, NJ (http://www.rcsb.org/).

[1] Present address: Institute of Biophysics, Chinese Academy of Sciences.

[2] To whom correspondence should be addressed. Tel.: 86-10-6275-5712; Fax: 86-10-6276-5913; E-mail: xiaofengz@pku.edu.cn.

[3] The abbreviations used are: TIM, triose-phosphate isomerase; BisTris, bis(2-hydroxyethyl)iminotris(hydroxymethyl)methane; ITC, isothermal titration calorimetry; NAG, *N*-acetyl-D-glucosamine; SI-CLP, stabilin-1 interacting chitinase-like protein.

alignment suggested conserved aromatic residues in the saccharide-binding cleft. Biochemical characterization revealed a binding property of SI-CLP with various saccharides. Further isothermal titration calorimetry (ITC) analysis identified GlcNAC polymer as the preferred polysaccharide. Site-directed mutagenesis of the conserved aromatic residues in the saccharide-binding cleft showed that mutation of these key residues abrogated saccharide-binding ability dramatically. Moreover, the binding ability of SI-CLP to lipopolysaccharide (LPS) was shown for the first time. The neutralization property of SI-CLP to LPS-induced inflammation was seen in further investigations. Our work provides structural basis for biological function of SI-CLP; subsequent study suggests the role of SI-CLP in microbe infection and inflammation.

MATERIALS AND METHODS

Cloning, Expression, and Purification of Recombinant SI-CLP—The cDNA encoding SI-CLP was cloned into a pET21DEST vector with an N-terminal His_6 tag. The first 22 residues (the signal peptide) of the protein were removed to obtain soluble expressed SI-CLP protein in *Escherichia coli* (9). Native or selenium-labeled SI-CLP was expressed in *E. coli* strain BL21(DE3) or B834(DE3), respectively, and purified as described previously (10). Purified SI-CLP protein used to treat cells was incubated with cleaned polymyxin B-agarose (Sigma) overnight to remove the endotoxin.

To identify key residues that participate in saccharide binding, we designed and constructed various mutants, Y84S, W88A, W110A, Y261S, W277A, Y302S, W380A, based on the structure superimposition of the SI-CLP and HCgp39·*N*-acetyl-D-glucosamine (NAG) complex (1LG1). Specific sites were mutated to Ala or Ser by overlap extension PCR. Mutated DNAs were inserted into pET28a vector and confirmed by DNA sequencing. The mutant proteins were expressed in BL21(DE3) and purified except W380A, which is insoluble.

Crystallization and Structure Determination—Recombinant SI-CLP proteins were purified using a procedure described previously (9) and crystallized using the sitting-drop method in a solvent of 100 mM BisTris (pH 6.5), 2 M $(NH_4)_2SO_4$, 10 mM 2-methyl-2,4-pentanediol, 100 mM $MgCl_2$. During data collection, the crystal was maintained at 100 K using nitrogen gas, with 20% glycerol as the cryoprotectant. X-ray diffraction data were collected on a MAR 325 CCD detector as 1° frames. The data were then processed using the programs of Mosflm and CCP4 package (11, 12). The crystallographic parameters and data collection statistics are given in Table 1.

The structure of SI-CLP was solved by the selenium single-wavelength anomalous dispersion method (Protein Data Bank accession no. 3BXW). The selenium sites were determined with PHENIX software (13) using data from 30 Å to 3 Å. Structure refinement was performed with program CNS (14) while being monitored by the R_{free} factor and the quality of the electron density maps. About half of the amino acids were autotraced by PHENIX, and the rest of SI-CLP structure was built manually, using Coot (15). The final structures were analyzed by MOLPROBITY and PROCHECK (16). The structure and figure were visualized using PyMOL and Coot. Ramachandran plots of the structures showed that 96.1% and 3.9% of residues are in the favored and allowed regions for SI-CLP structure, respectively, and no residues are in the generally allowed and disallowed regions.

TABLE 1
Data collection and refinement statistics for SI-CLP structure

Space group	$P3_221$
Unite cell *a*, *b*, *c* (Å)	100.1, 100.1, 250
Resolution (Å)	50-2.7 (2.85-2.7)[a]
Reflections, unique/total observed	40,781/301,288
Completeness (%)	99.9 (100)
Multiplicity	6.6
$I/\sigma(I)$	15.1 (2.5)
R_{merge}[b]	0.127 (0.751)
R_{pim} (within $I+/I-$)[c]	0.058 (0.272)
R_{work}	22.23
R_{free}[d]	25.29
Model	
No. atoms	5,880
Water molecules	16
Solvent content (%)	69.38
Overall *B* factor from Wilson plot	44.6
Root mean square difference	
Bonds (Å)	0.01
Angles (°)	1.4
Ramachandran plot (%)	
Favored region	96.1
Additionally allowed region	3.9

[a] Values in parentheses are for highest resolution shell.
[b] $R_{merge} = \Sigma h \Sigma i |Ii(h) - <I(h)>| / \Sigma h \Sigma i Ii(h)$.
[c] $R_{pim} = \Sigma h (1/(N-1))1/2 \Sigma i |Ii(h) - <I(h)>| \Sigma h \Sigma i Ii(h)$.
[d] $R_{work} = \Sigma h ||F_o|h - |F_c|h| / \Sigma h F_o|h$. R_{free} corresponds to R_{work} calculated using 5% of the total reflections selected randomly in thin shells and excluded during refinement. *I* is the observed intensity, and $<I>$ is the average intensity of multiple observations from symmetry-related reflections. F_o and F_c are the observed and calculated structure factors, respectively.

Detection of SI-CLP-Binding Property—BIAcore 3000 (Amersham Pharmacia Biosciences) was first used to screen for the binding specificity of SI-CLP to various monosaccharides, including GlcN, GalN, *N*-acetylglucosamine (GlcNAc), *N*-acetylgalactosamine (GalNAc), mannose, glucose, and ribose (Sigma). Purified SI-CLP (200 μg/ml) in 10 mM sodium acetate (pH 5.0) or control buffer was immobilized separately onto the surface of sensor chip CM5 (Amersham Pharmacia Biosciences) activated with primary amines. Excess *N*-hydroxysuccinimide ester groups were blocked by 1 M ethanolamine hydrochloride. Monosaccharides and LPS in HBS buffer (10 mM HEPES with 150 mM NaCl, 3 mM EDTA, and 0.05% Tween 20) were injected across the surface at a flow rate of 30 μl/min, and real-time binding curves were observed. To stop the reaction, HBS-ET buffer was introduced onto the sensor chip to start the dissociation. The bulk effect of refractive index changes was subtracted from the in-line reference flow cell to yield true binding response. Kinetic data were calculated using the BIA evaluation software 4.1 (Pharmacia Biosensor AB).

To measure accurately the binding intensity of SI-CLP to saccharides further, ITC analysis was performed to compare the binding activity of SI-CLP with polysaccharides of different lengths (see Fig. 4*C*). The binding constant of wild-type SI-CLP and its mutants to polysaccharides was measured by monitoring the heat change using the VP-ITC Micro Calorimeter (MicroCal, Inc.). The sample cell was filled with 100 μM protein, and the injection syringe was filled with 10 mM polysaccharides. Both the protein and polysaccharides were dissolved in the buffer containing 10 mM Tris, 200 mM NaCl (pH 8.0); measurements were carried out at 25 °C. Heat change upon the addition of substrate solution was monitored, and the ITC data

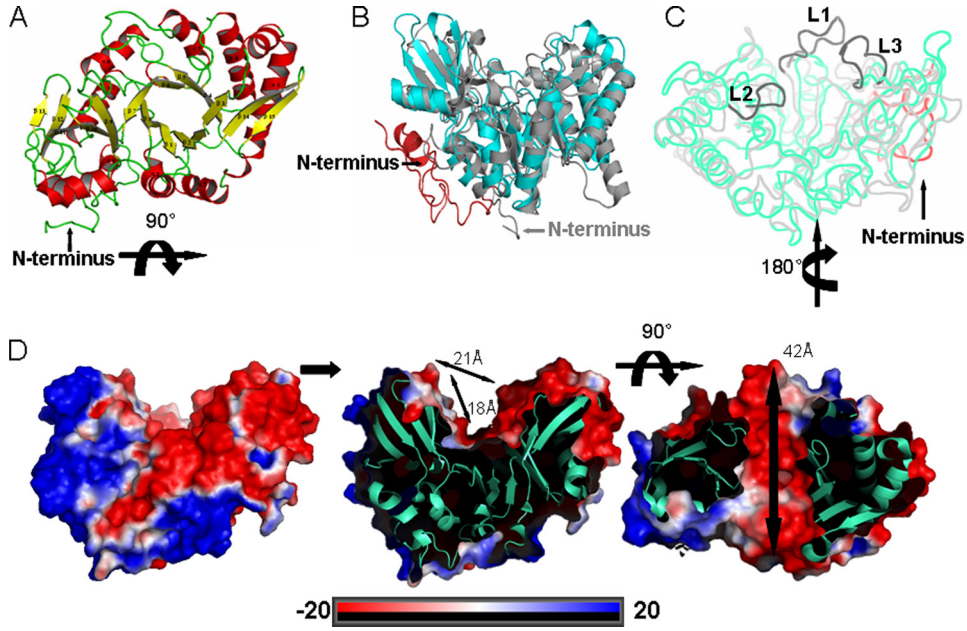

FIGURE 1. **Overall structure of SI-CLP.** *A*, ribbon diagram of SI-CLP with labeled secondary structural element. The structure shows a typical TIM barrel fold with eight-stranded parallel β-barrel surrounded by eight α-helices antiparallel to the barrel. This figure and the following structural drawings were prepared with PyMOL. *B*, superimposition of SI-CLP (*cyan*, PDB accession no. 3BXW) and YM1 (*gray*, PDB accession no. 1VF8). YM1 is a secretory protein synthesized by activated murine peritoneal macrophages; it is recognized as a novel mammalian lectin with a binding specificity to GlcN. The novel structural motif in the N terminus of SI-CLP is labeled in *red*. *C*, ribbon structure showing alignment between SI-CLP (*gray*) and HCgp39 (*green-cyan*). Three loops (labeled *L1*, *L2*, and *L3*) that do not exist in SI-CLP but are found in other Glyco_18 chitinase-like proteins are colored *deep gray*. The absence of these loops in SI-CLP leads to the uncharacterized open cleft. *D*, *saddle-shaped cleft* in two views represented by surface electrostatic potential. The *cut-through* SI-CLP section indicates the shape and surface features of the cleft.

TABLE 2
Comparison of SI-CLP with chitotriosidase or chitinase-like proteins

	Sequence identity	Root mean square difference	Length of Glyco_18 domain (amino acids)	Conserved motif	Enzyme activity
	%				
Chitotriosidase	100	0	366 (22–387)	D*X*X*D*X*D*X*E*	Detectable
HCgp39	55	1	362 (22–383)	D*X*X*D*X*A*X*L*	NA[a]
YM1	49	0.8	373 (22–395)	D*X*X*N*X*D*X*Q*	NA
SI-CLP	18	2.3	316 (77–392)	D*X*X*V*X*E*X*W*	NA

[a] NA indicates that there is no glycosyl hydrolase activity.

were fit using a one-set-of-sites model. The binding constant was calculated using the software provided by the manufacturer (MicroCal, Inc.).

Cell Culture and Treatment—Cell lines used in the experiment were maintained at 37 °C with 5% CO_2 in RPMI medium 1640 (Invitrogen) supplemented with 10% fetal calf serum (FCS; Hyclone) without antibiotics. Monocytic THP-1 cells were treated with 50 ng/ml phorbol 12-myristate 13-acetate (Sigma) for 48 h and differentiated into a macrophage-like phenotype that closely resembles human monocyte-derived macrophages. To examine the effect of neutralization of SI-CLP on the production of LPS-induced inflammatory cytokines, the THP-1 macrophages were stimulated with 10 μg/ml SI-CLP and 1 μg/ml LPS for 24 h. Control groups in the *in vitro* assay were treated with heated-denatured protein or PBS buffer. Cells were then harvested, and the total RNA was isolated using TRIzol reagent (Invitrogen) according to the manufacturer's protocol.

Real-time Quantitative RT-PCR Analysis—Using 1 μg of total RNA, we generated cDNA with the RT system (Promega) following the manufacturer's protocol. The mRNA expression levels of proinflammation factors (IL-1β, IL-8, TNFα, and IL-6) were examined by real-time quantitative RT-PCR with the SYBR Green qPCR kit (Finnzymes) in a DNA Engine Opticon continuous fluorescence detection system (MJ Research). β-Actin was used to correct for intersample variations.

RESULTS

Overall Structure of SI-CLP—The structure of full-length SI-CLP was determined by selenium single-wavelength anomalous dispersion method and refined against 2.7 Å diffraction data, to a final *R* factor (R_{free}) of 25.29 with good stereochemistry (Table 1 and Fig. 1). Despite its low sequence identity to other structure-known proteins, SI-CLP adopts a classical Glyco_18 chitinase fold consisting of two domains (Table 1 and supplemental Fig. 1). The core domain contains a typical TIM barrel fold with eight-stranded parallel β-barrel surrounded by eight α-helices antiparallel to the barrel (Fig. 1*A*). An additional glove-like $\alpha+\beta$ domain (residues 298–354), composed of one α-helix (α10) and five antiparallel β-strands (β11–15), is inserted between strand β10 and helix α9 (supplemental Fig. 1). Structure comparisons with other TIM barrel glycosyl hydrolases revealed that the conserved aspartic acids in the motif D*X*X*D*X*D*X*E, essential to the glycosyl hydrolase activity, are replaced by valine or glutamic acid in SI-CLP (Table 2). This may explain the loss of glycosyl hydrolase activity in SI-CLP.

Although SI-CLP adopts typical TIM barrel folding, it has a lower structure similarity to any other TIM-fold proteins with a root mean square difference of 2.3Å to chitotriosidase that has a structure that is most similar to SI-CLP. The structure of SI-CLP differs from the other Glyco_18 chitinase-like proteins in following two aspects. First, the most notable difference between SI-CLP and the other Glyco_18 chitinase family proteins is the existence of an additional helix region with fewer secondary structural elements at the N terminus of SI-CLP (residues 22–78) (Fig. 1*B*). This structural motif is composed of a short α-helix (residues 53–62) flanked by nonstructured loops on both sides (Fig. 1*B* and supplemental Fig. 1). In addition, a short helix near the C terminus (α11) and a positive-charge-rich area are buried by the N-terminal motif. A free cysteine exposed to the surrounding solvent is also observed in the structure of SI-CLP, but not in the other Glyco_18 family proteins. Second, compared with other Glyco_18 chitinase-like

proteins, SI-CLP has a shorter Glyco_18 domain (Table 2), which we can recognize from the gaps in the sequence alignment (supplemental Fig. 1). SI-CLP also contains a more open binding cleft that is different from the binding cleft for $GlcNAc_8$ found in human cartilage glycoprotein (HCgp39, also named YKL40) (3, 4) (Figs. 1*C* and 2).

The cleft of SI-CLP is saddle-shaped and measures ~18 Å in depth, 21 Å in width, and 42 Å in length (Fig. 1*D*). Comparisons of its main chain tracing with that around the saccharide-binding clefts in other proteins revealed that there are three loops restricting the capacity of the cleft. One is the loop between β1 and α2 in the TIM barrel (L1), which is shorter and more rigid in SI-CLP compared with that of HCgp39 (supplemental Figs. 1 and 2). The second one is the loop between β6 and α4 (L2). The main chain of α4 in SI-CLP moves 3 Å away from the β-sheet barrel and results in an extension of this loop. The third loop (L3), which is located between β10 and β11 in the inserted $\alpha+\beta$ domain of HCgp39 and other chitinase-like proteins, does not exist in SI-CLP (β12; Fig. 1*C* and supplemental Fig. 2). All of these characteristics make the cleft in SI-CLP widely open (Fig. 2), suggesting that this cleft holds different sugar-binding properties than do other chitinase-like proteins.

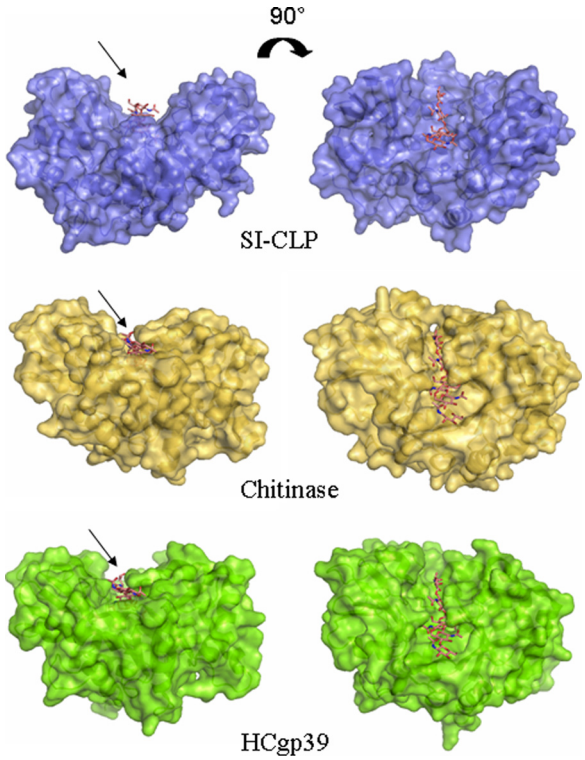

FIGURE 2. **Structural comparison of SI-CLP with other chitinases reveals an open binding cleft of SI-CLP.** SI-CLP surface structure (*slate*) is compared with chitotriosidase (1HKK, *yellow-orange*) and HCgp39 (1HJW, *splitpea*). The chitooligosaccharides NAG6 are shown as *sticks*. The *arrow* shows the widened cleft of SI-CLP.

Identification of a Putative Saccharide-binding Site in SI-CLP—Although sequence alignment between SI-CLP and other chitinase-like proteins revealed no information of the conserved residues, superimposition of the structures of SI-CLP and HCgp39·NAG) complex (1LG1) showed that SI-CLP has a similarly shaped cleft; structure superimposition-based sequence alignment identified the conserved solvent-exposed aromatic residues including Tyr-84, Trp-88, Trp-110, Tyr-261, Tyr-302, and Try-380 on the surface of the binding pocket (Fig. 3*A*). These residues are highly conserved in other chitinase-like proteins and are important for interacting with the hydrophobic faces of the pyranose rings in chitooligosaccharides (3, 4, 17).

Electrostatic surface potential calculations for SI-CLP and NAG_6 positioned into the cleft were performed to help us further understand possible interactions between glycosaminoglycan and SI-CLP. The surface of the possible substrate-binding cleft of SI-CLP showed an electronegative potential (*red*, Fig. 3*B*), which is appropriate for a positively charged substrate such as NAG_6 and could explain why the sugar ring of the NAG_6 can fit snugly into the open cleft of SI-CLP (Fig. 3).

Saccharide Binding of SI-CLP—The open cleft in SI-CLP inspired us to explore its saccharide-binding property. GlcN and GalN were shown to bind specifically to SI-CLP in a concentration-dependent manner (Fig. 4*A*). GalNAc and GlcNAc could bind to SI-CLP as well. Ribose and mannose could also bind to SI-CLP to some extent, whereas glucose and galactose did not show any binding (Fig. 4*A*).

Because all chitinase-like proteins bind preferentially to saccharides polymers, we further examined the binding activity of SI-CLP to various polysaccharides of different lengths using ITC analyses (Fig. 4*B*). The binding activity of SI-CLP to GlcN trimer was examined first. Interestingly, although SI-CLP binds GlcN with high affinity (Fig. 4*A*), the binding of GlcN trimer to the protein is weak. The binding of different lengths of GlcNAC polymer to SI-CLP was then investigated. The K_a values of different GlcNAC polymers binding to SI-CLP were calculated and compared (Fig. 4*C*). The GlcNAc tetramer has the highest affinity compared with the trimer and pentamer. These results suggest that SI-CLP prefers to bind oligosaccharides with a four-sugar ring core,

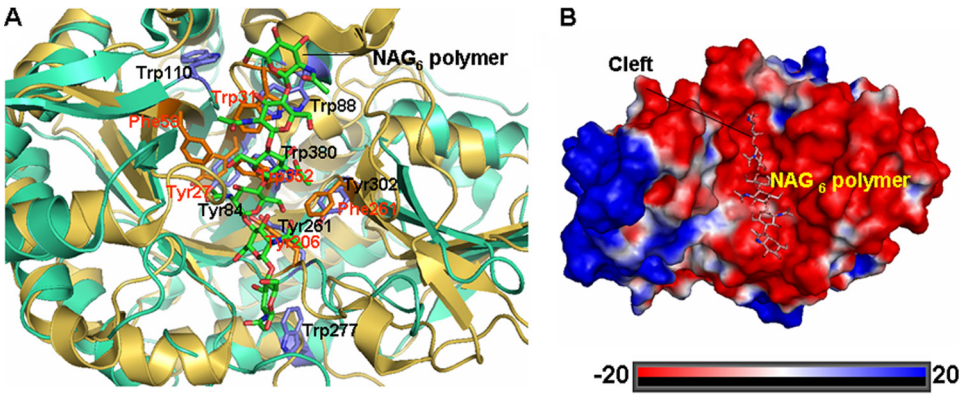

FIGURE 3. **Model of ligands binding to SI-CLP.** *A*, superimposition of SI-CLP and HCgp39·NAG complex (1LG1) showing the saccharide-binding cleft. The NAG_6 is shown as *sticks*. The SI-CLP backbone is shown in *green-cyan*, and the HCgp39 complex is shown in *bright orange*. *B*, molecular surface (calculated with PyMOL, positive in *blue*, 20 kT, negative in *red*, −20 kT) for SI-CLP docked with NAG_6.

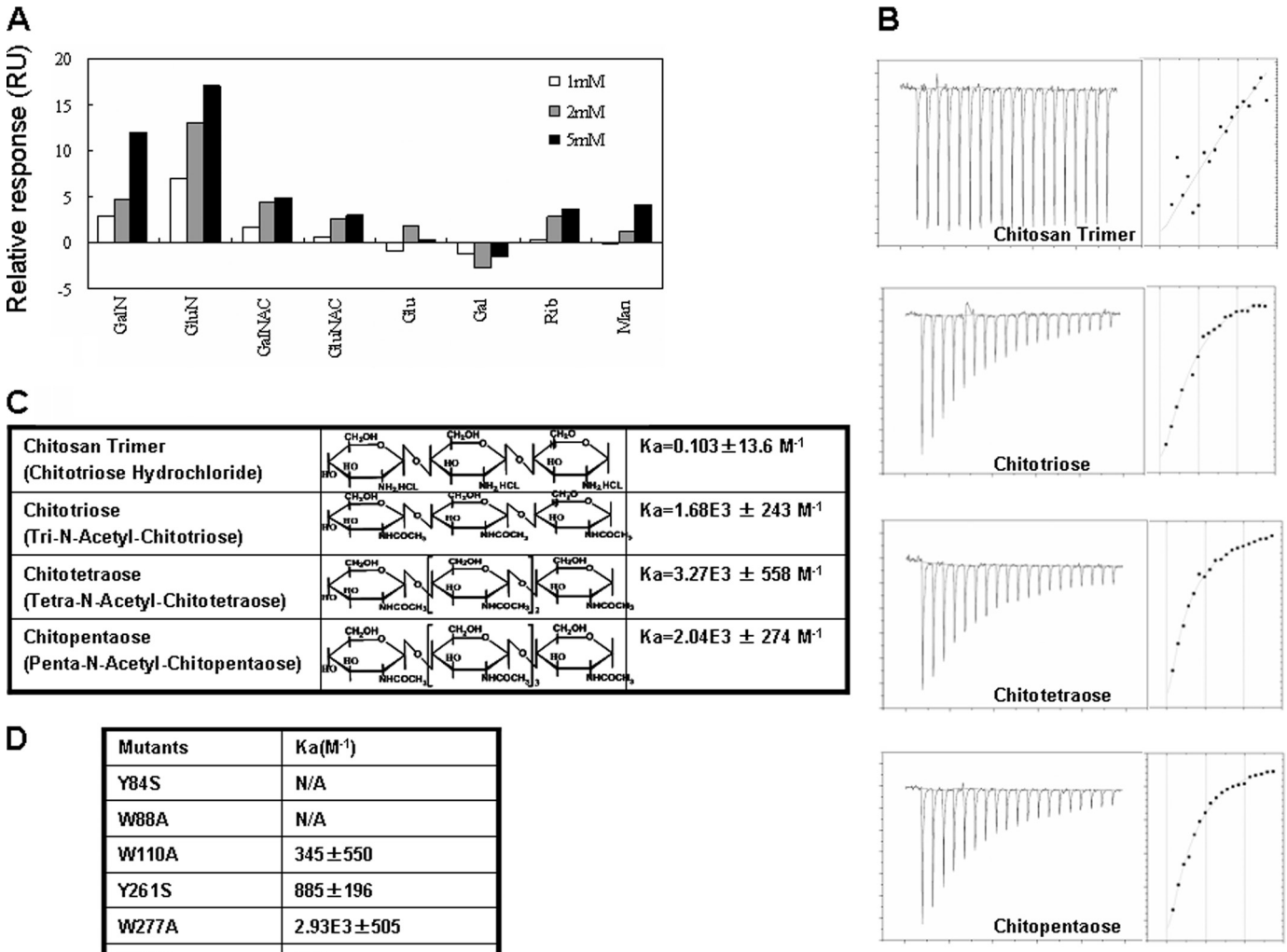

Mutants	Ka(M^{-1})
Y84S	N/A
W88A	N/A
W110A	345±550
Y261S	885±196
W277A	2.93E3±505
Y302S	N/A

FIGURE 4. **Binding of saccharides to SI-CLP.** *A*, surface plasmon resonance analyses showed the binding of various monosaccharides to SI-CLP and suggest that GlcN and GalN are the preferred monosaccharide ligands to SI-CLP. *B*, ITC analyses showed the binding of polysaccharides to SI-CLP. *C*, calculated association constant of each polysaccharide to SI-CLP is shown. *D*, mutation of the aromatic residues on the cleft surface significantly decreased the binding activity of protein to tetra-GlcNAC. Several mutants of SI-CLP protein were designed and purified; the K_a of these mutants binding to NAG4 was calculated through ITC analyses. *N/A* stands for no sugar-binding activity detected for these mutants, which the $K_a \ll 10^{-1}$.

which is similar to YKL40 (3). Furthermore, the association constant (K_a) of SI-CLP to tetra-GlcNAC is $3.27 \times 10^3\ M^{-1}$, which is comparable with the K_a of YM1 binding to tetra-GlcN ($3.36 \times 10^3\ M^{-1}$) (6).

To identify further the key residues that are essential for carbohydrate binding, the aromatic residues located around the surface of the binding pocket, Tyr-84, Trp-88, Trp-110, Tyr-261, Trp-277, and Tyr-302 were mutated to either Ala or Ser and then purified and their binding activities to the tetra-GlcNAC measured by ITC. The result showed that the mutants of the aromatic residues on the cleft surface all significantly decreased binding activity to tetra-GlcNAC, but the mutant of the aromatic residues Trp-277 far from the sugar and not conserved in other chitinase like protein did not severely decrease the binding activity (Fig. 4*D*). These data indicate that these conserved aromatic residues are the key residues contributing to the interactions for carbohydrate binding and that the open cleft of SI-CLP is the sugar-binding site, as with other chitinase-like proteins.

Neutralization of LPS Effects by SI-CLP—Because SI-CLP shows no tightly restricted sugar-binding property with a wide binding cleft, we assumed that the wider cleft could adopt various types of sugar and has no specific sugar-binding property. LPS is a potent microbial initiator of inflammation containing oligosaccharide core (18–20). We further measured the ability of SI-CLP (0.2 μg/μl) to bind different concentrations of LPS (0.0015 μg/μl, 0.03 μg/μl, 0.06 μg/μl, 0.12 μg/μl, 0.25 μg/μl) and found clearly that SI-CLP could bind LPS in a concentration-dependent manner (Fig. 5*A*).

The effect of SI-CLP on LPS-stimulated inflammation reaction was further investigated. Phorbol 12-myristate 13-acetate-differentiated THP-1 macrophages were treated with 1 μg/ml LPS in the absence or presence of 10 μg/ml recombinant SI-CLP proteins, and the expression of proinflammatory cytokines IL-1β, IL-8, TNFα, and IL-6 was measured. LPS did stimulate the production of the cytokines in the presence of only self-secreted SI-CLP alone, but incubation with recombinant SI-CLP significantly decreased production of proinflammatory

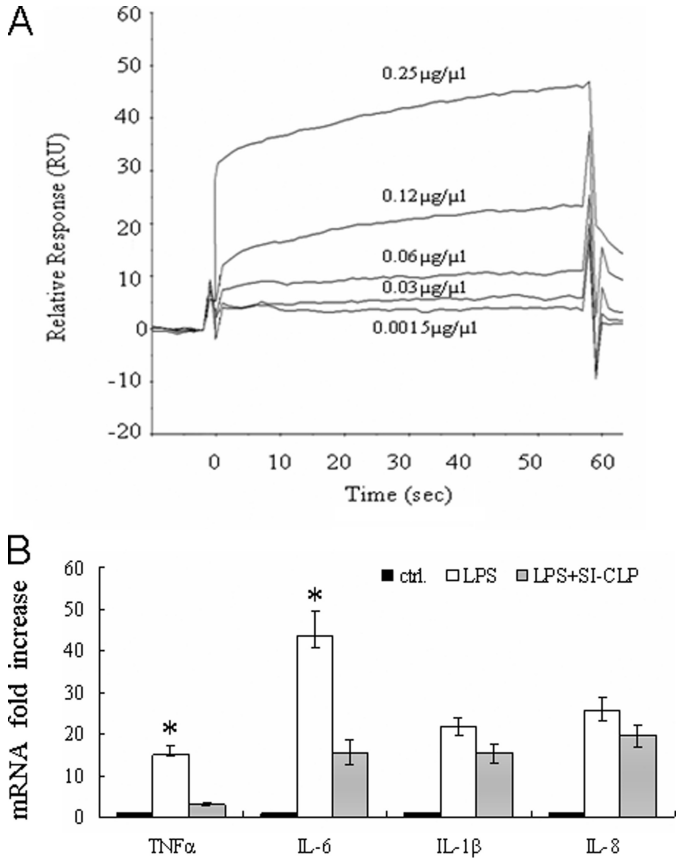

FIGURE 5. **Effects of recombinant SI-CLP binding to LPS.** *A*, surface plasmon resonance analyses confirmed the binding of LPS to SI-CLP. Binding of different concentrations of LPS, 0.0015, 0.03, 0.06, 0.12, and 0.25 μg/μl, to SI-CLP (0.2 μg/μl) were examined as described under "Materials and Methods." *B*, level of TNFα, IL-6, IL-1β, or IL-8 induced by LPS (1 μg/ml) in phorbol 12-myristate 13-acetate-differentiated THP-1 macrophages was significantly reduced when excessive amounts of recombinant SI-CLP (10 μg/ml) were added in the culture medium compared with that in the presence of only self-secreted SI-CLP. The results are means $\pm$ S.D. (*error bars*) of four independent experiments. The *p* value (*, $p < 0.01$, cells treated with LPS and SI-CLP were compared with cells treated only with LPS) was ascertained by Student's *t* test.

factors TNFα, IL-6, IL-1β, and IL-8 (Fig. 5*B*). Apparently, binding of SI-CLP with LPS could negate the endotoxin effects induced by LPS on macrophages.

DISCUSSION

Members of the Glycol_18 family have been studied because of their functions in the immune system. Acidic mammalian chitinase has chitinase activity and was identified as a mediator of IL-13-induced responses in Th2-dominated disorders such as asthma (1). YM1 reportedly binds GlcN oligomer and is regulated by Th2 cytokines; it is abundantly expressed in macrophages of Th2 chronic inflammation (21). Crystal structures of chitotriosidase, HCgp39 (YKL40), and YM1 show that they have a highly conserved TIM barrel fold with a saccharide-binding cleft (2–5, 17), suggesting that proteins containing this conserved fold could carry similar functions.

As a novel chitinase-like protein, SI-CLP was found to be regulated by Th2 cytokines (8), as with acidic mammalian chitinase and YM1. Similar to other chitinase-like protein, SI-CLP is also expressed abundantly in macrophages. Besides, SI-CLP has also been found to be up-regulated in patients with chronic inflammatory disorders of the respiratory tract, human peripheral blood leukocytes (8), osteoarthritis, and rheumatoid arthritis. These data suggest that SI-CLP might involve in innate immunity. However, the physiology function of SI-CLP has remained largely unknown. The crystal structure of SI-CLP was determined here to find clues to its function; biochemical characterization of binding of SI-CLP to saccharides demonstrated that SI-CLP belongs to the Glycol_18 domain-containing family, but has much more structure variations.

The crystal structure of SI-CLP adopts the classical TIM barrel fold with a longer and flattened negatively charged cleft, suggesting diversified ligand recognition of SI-CLP. In comparing binding by different monosaccharides to SI-CLP using SPR analysis, the best binding substrate we tested is GlcN; however, further ITC analysis revealed that for saccharide polymers, GlcNAC tetramer has the highest binding activity, indicating that the four-sugar ring core has the best affinity to SI-CLP. GlcNAC is the component of chitin which is the antigen of fungus and parasites. Considering the sugar-binding diversity of SI-CLP, we therefore tried to ascertain whether SI-CLP could bind LPS, which is composed of a sugar core and lipid chain and is a kind of antigen from Gram-negative microbes. Indeed, binding of SI-CLP to LPS was confirmed by SPR analysis (Fig. 5*A*). The binding of LPS by SI-CLP consequently negates the LPS-induced endotoxin effect (Fig. 5*B*). This is the first time that binding of LPS to chitinase-like protein has been identified in a macrophage-associated protein.

Considering the low binding activity of SI-CLP to LPS *in vitro*, we presume that neutralization of LPS-induced effects by SI-CLP is through binding to LPS or manipulating a signaling pathway, or a combined effect. The argument that SI-CLP could not neutralize LPS effects under physiological conditions due to a low *in vitro* affinity to LPS is based on the assumption that SI-CLP may neutralize LPS effects only by physically binding LPS and then neutralizing its effects. Because we do not know how SI-CLP neutralizes LPS effects *in vivo*, we could only speculate. How much of a role LPS binding by SI-CLP is in this process *in vivo* could not be defined quantitatively right now. In addition, we must consider the roles of other factors. For instance, other proteins that associate with SI-CLP *in vivo* may increase its affinity to LPS. Besides, overlapping signal pathways and other factors may also affect SI-CLP functions *in vivo*. The affinity of SI-CLP to LPS may help to recruit SI-CLP to the inflammatory site, even though SI-CLP might not be able to inhibit LPS completely by direct binding. We suggest that inhibition of LPS-induced IL-1β and other cytokines by SI-CLP may be either through directly blocking the LPS binding or by affecting a signal pathway.

Accumulated data have shown that chitinase-like proteins lacking enzymatic activity are possibly involved in host defense against chitin-containing pathogens. Unlike other chitinase-like proteins that have tight ligand-binding restrictions, we found here for the first time that SI-CLP bind ligands with less selectivity, and in addition to chitin, SI-CLP could neutralize LPS-induced immune responses as well. These results suggest that SI-CLP could not only sense chitin-containing pathogens as do other chitinase-like proteins, but also could neutralize

LPS-induced endotoxin effects through either its binding to the sugar moiety in LPS or other unknown mechanisms. Because of the association between chitinase-like proteins and immune diseases (1, 22), further investigation is in progress to establish in detail the mechanism of SI-CLP in regulation of macrophage inflammation and the roles that SI-CLP may play in immune disorders.

Acknowledgments—We thank Professors Xiaocheng Gu and Yicheng Dong for critical reading of the manuscript, and we acknowledge the technical assistance of Xinping Liu.

REFERENCES

1. Zhu, Z., Zheng, T., Homer, R. J., Kim, Y. K., Chen, N. Y., Cohn, L., Hamid, Q., and Elias, J. A. (2004) *Science* **304,** 1678–1682
2. Fusetti, F., von Moeller, H., Houston, D., Rozeboom, H. J., Dijkstra, B. W., Boot, R. G., Aerts, J. M., and van Aalten, D. M. (2002) *J. Biol. Chem.* **277,** 25537–25544
3. Fusetti, F., Pijning, T., Kalk, K. H., Bos, E., and Dijkstra, B. W. (2003) *J. Biol. Chem.* **278,** 37753–37760
4. Houston, D. R., Recklies, A. D., Krupa, J. C., and van Aalten, D. M. (2003) *J. Biol. Chem.* **278,** 30206–30212
5. Sun, Y. J., Chang, N. C., Hung, S. I., Chang, A. C., Chou, C. C., and Hsiao, C. D. (2001) *J. Biol. Chem.* **276,** 17507–17514
6. Chang, N. C., Hung, S. I., Hwa, K. Y., Kato, I., Chen, J. E., Liu, C. H., and Chang, A. C. (2001) *J. Biol. Chem.* **276,** 17497–17506
7. Kzhyshkowska, J., Gratchev, A., and Goerdt, S. (2007) *Biomark. Insights* **2,** 128–146
8. Kzhyshkowska, J., Mamidi, S., Gratchev, A., Kremmer, E., Schmuttermaier, C., Krusell, L., Haus, G., Utikal, J., Schledzewski, K., Scholtze, J., and Goerdt, S. (2006) *Blood* **107,** 3221–3228
9. Dai, X., Chen, Q., Lian, M., Zhou, Y., Zhou, M., Lu, S., Chen, Y., Luo, J., Gu, X., Jiang, Y., Luo, M., and Zheng, X. (2005) *Biochem. Biophys. Res. Commun.* **332,** 593–601
10. Meng, G., Bai, X., Green, T. J., Luo, M., and Zheng, X. (2009) *Protein Pept. Lett.* **16,** 336–338
11. Powell, H. R. (1999) *Acta Crystallogr. D Biol. Crystallogr.* **55,** 1690–1695
12. Collaborative Computational Project Number 4 (1994) *Acta Crystallogr. D Biol. Crystallogr.* **50,** 760–763
13. Adams, P. D., Grosse-Kunstleve, R. W., Hung, L. W., Ioerger, T. R., McCoy, A. J., Moriarty, N. W., Read, R. J., Sacchettini, J. C., Sauter, N. K., and Terwilliger, T. C. (2002) *Acta Crystallogr. D Biol. Crystallogr.* **58,** 1948–1954
14. Brünger, A. T., Adams, P. D., Clore, G. M., DeLano, W. L., Gros, P., Grosse-Kunstleve, R. W., Jiang, J. S., Kuszewski, J., Nilges, M., Pannu, N. S., Read, R. J., Rice, L. M., Simonson, T., and Warren, G. L. (1998) *Acta Crystallogr. D Biol. Crystallogr.* **54,** 905–921
15. Emsley, P., and Cowtan, K. (2004) *Acta Crystallogr. D Biol. Crystallogr.* **60,** 2126–2132
16. Laskowski, R. A., Rullmannn, J. A., MacArthur, M. W., Kaptein, R., and Thornton, J. M. (1996) *J. Biomol. NMR* **8,** 477–486
17. Rao, F. V., Houston, D. R., Boot, R. G., Aerts, J. M., Sakuda, S., and van Aalten, D. M. (2003) *J. Biol. Chem.* **278,** 20110–20116
18. Beutler, B., and Rietschel, E. T. (2003) *Nat. Rev. Immunol.* **3,** 169–176
19. Cohen, J. (2002) *Nature* **420,** 885–891
20. Raetz, C. R. (1990) *Annu. Rev. Biochem.* **59,** 129–170
21. Welch, J. S., Escoubet-Lozach, L., Sykes, D. B., Liddiard, K., Greaves, D. R., and Glass, C. K. (2002) *J. Biol. Chem.* **277,** 42821–42829
22. Steenbakkers, P. G., Baeten, D., Rovers, E., Veys, E. M., Rijnders, A. W., Meijerink, J., De Keyser, F., and Boots, A. M. (2003) *J. Immunol.* **170,** 5719–5727